https://doi.org/10.15407/ujpe64.10.942

A.M. POGORILY,[1] D.M. POLISHCHUK,[1] A.I. TOVSTOLYTKIN,[1] A.F. KRAVETS,[1] V.O. ZAMORSKYI,[1] A.V. NOSENKO,[2] V.K. NOSENKO[2]

[1] Institute of Magnetism, Nat. Acad. of Sci. of Ukraine
and Ministry of Education and Science of Ukraine
(36b, Academician Vernadsky Blvd., Kyiv 03142, Ukraine; e-mail: kravets@imag.kiev.ua)
[2] G.V. Kurdyumov Institute for Metal Physics, Nat. Acad. of Sci. of Ukraine
(36, Academician Vernadsky Blvd., Kyiv 03142, Ukraine)

RESONANCE PROPERTIES AND MAGNETIC ANISOTROPY OF NANOCRYSTALLINE $Fe_{73}Cu_1Nb_3Si_{16}B_7$ ALLOY

Resonance properties of nanocrystalline ribbons of $Fe_{73}Cu_1Nb_3Si_{16}B_7$ alloy annealed with the use of an electric current under a tensile stress of 180 MPa have been studied within the ferromagnetic resonance method. Two kinds of ferromagnetic regions with different anisotropic behaviors that coexist in the alloy after the annealing are detected. One of them is amorphous and weakly magnetically anisotropic, whereas the other is characterized by a pronounced uniaxial magnetic anisotropy and corresponds to the nanocrystalline phase. Quantitative estimations of magnetic parameters in two magnetic phases of the alloy are made.

Keywords: ferromagnetic resonance, amorphous ribbon, nanocrystalline alloy, magnetic anisotropy.

1. Introduction

Nowadays, soft magnetic nanocrystalline alloys belonging to the Fe-Nb-Cu-Si-B system [1] are widely used in magnetic circuits of various inductive components (transformers and chokes). The formation of α-Fe(Si) nanocrystals in those alloys under their heat treatment is known to improve their soft magnetic characteristics. After a graduated annealing, the volume fraction of the nanocrystalline phase in those alloys is about 80%, with the average size of nanocrystallites varying from 10 to 12 nm [1–5]. In the alloys of this type, the shape of a hysteresis loop can be changed by inducing the uniaxial magnetic anisotropy making use of either the annealing in an external magnetic field [6–8] or annealing under tensile stresses [9–12].

Magnetic circuits with a pronounced magnetic anisotropy possess a number of advantages. The main of them are the high-frequency stability of the magnetic permittivity [13, 17] and low losses in the most widely used frequency interval ranging from 10 to 100 kHz [13–17]. Those advantages attract a considerable interest to the conditions and possibilities of the formation of the transverse magnetic anisotropy in nanocrystalline alloys in order to obtain the highest possible magnetic characteristics. Therefore, extended studies of the magnetic resonance are required for understanding the behavior of the nanocrystalline and residual amorphous phases that are formed in nanocrystalline alloys after their annealing.

The rapid heating of an amorphous ribbon, which was fabricated from $Fe_{73}Cu_1Nb_3Si_{16}B_7$ alloy in the course of its isothermal annealing making use of the electric current induces the appearence of a magnetic anisotropy in this ribbon, which is transverse to the current direction [18]. The origin of this phenomenon has been poorly examined. One of its possible origins can be the formation of various magnetic phases with an induced magnetic anisotropy in the amorphous matrix during the annealing of this amorphous alloy. In order to detect such phases, the ferromagnetic resonance (FMR) method is used in this work. This method makes it possible to detect the presence of various magnetic phases in multicomponent alloys with high efficiency and to obtain the information about magnetic parameters of those phases. Accordingly, the resonance properties

of $Fe_{73}Cu_1Nb_3Si_{16}B_7$ alloy ribbons are studied, and the magnetic anisotropy constant K_u of this nanocrystalline alloy after the isothermal annealing with the help of an electric current is evaluated.

2. Experimental Samples and Methods

The amorphous alloy $Fe_{73}Cu_1Nb_3Si_{16}B_7$ MELTA® MM-11N (hereafter, MM-11N) was obtained in the form of a ribbon 20 μm in thickness and 10 mm in width by casting a flat melt flow. After its melting in a quartz tube (a melt temperature of 1400 °C) and in a protective atmosphere of carbon dioxide, the alloy was planarly poured under a pressure of 20 kPa onto a chrome bronze wheel 620 mm in diameter through a narrow rectangular gap 0.4×10 mm^2 in size and located at a distance of 0.2 mm from the wheel, which rotated at a linear velocity of 25 m/s. The ultrarapid cooling of a melt resulted in the formation of a ribbon of the amorphous $Fe_{73}Cu_1Nb_3Si_{16}B_7$ alloy.

The transverse magnetic anisotropy was induced in the amorphous MM-11N ribbon by quickly crystallizing the latter in the air environment with the help of the high-rate ribbon heating for 3.7 s using the electric current with a density of 42 A/mm^2 and simultaneously stretching the ribbon along its axis with a stress of up to 180 MPa.

The ferromagnetic resonance spectra of the MM-11N ribbons were registered at room temperature and at a frequency of 9.45 GHz (the X-band) using an electron paramagnetic resonance spectrometer ELEXSYS-E500 (Bruker BioSpin GmbH, Germany). The application of an automatic goniometer made it possible to obtain the angular dependences of the resonance fields in two measurement configurations (Fig. 1). The effective magnetization of the ferromagnetic regions in MM-11N alloy, M_{eff}, was calculated from the FMR measurements using the Kittel system of equations [19]

$$\begin{aligned} \frac{\omega}{\gamma} &= H_{\perp} - 4\pi M_{\text{eff}}, \\ \frac{\omega}{\gamma} &= \sqrt{H_{\parallel}(H_{\parallel} + 4\pi M_{\text{eff}})}, \end{aligned} \tag{1}$$

where $H_{\perp}$ and $H_{\parallel}$ are resonance fields for the perpendicular and parallel, respectively, orientations of the magnetic field **H** with respect to the MM-11N ribbon plane, ω is the frequency of the applied ultrahigh-frequency magnetic field, and γ is the gyromagnetic ratio. The values of the parameters $H_{\perp}$, $H_{\parallel}$, ω, and

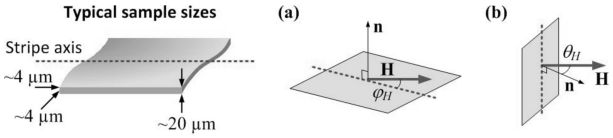

Fig. 1. Typical sizes of specimens studied for FMR and two measurement configurations with the magnetic field **H** applied (*a*) in the ribbon plane and (*b*) in the plane including the normal **n** to the ribbon surface and perpendicularly to the MM-11N ribbon axis (the ribbon axis is parallel to the direction of an electric current at the sample annealing)

γ were found experimentally. By analyzing the half-width of the FMR lines of magnetic phases, the information concerning the magnetic and structural heterogeneity of each phase was obtained. When doing so, the fact that the half-width of the FMR lines increases with the magnetic inhomogeneity in MM-11N alloy was taken into account.

It should be noted that the Kittel formulas are rigorously applicable only to an ellipsoid that is uniformly magnetized over its volume and is such that the microwave field in it is uniform. For metallic magnets, such conditions are satisfied, if the skin-layer depth exceeds the specimen thickness [20]. For specimens manufactured following the procedure described in this work, but subjected to the annealing for a time interval that was three times longer, the specific electrical resistance was equal to 1.16×10^{-6} Ω m [18]. The skin-layer depth is about 18 μm at a frequency of 9.45 GHz in this case. Since the shorter annealing times lead, as a rule, to the formation of specimens with higher specific resistances [18], the skin layer in the specimens examined in this work should be expected to exceed the specimen thickness (20 μm). Therefore, the application of Kittel equations (1) is correct in this case.

The obtained angular dependences of the resonance fields were analyzed on the basis of the Smit–Beljers FMR formalism [21] making use of the following expression for the free energy of a ferromagnetic alloy:

$$\begin{aligned} F = {} & \mathbf{MH} - 0.5MH_{\text{ua}}\cos\varphi\sin\theta + \\ & + 0.5M\,(4\pi M_{\text{eff}})\cos^2\theta. \end{aligned} \tag{2}$$

3. Results and their Discussion

In Fig. 2, the angular dependences of the FMR absorption spectra registered at the orientation of an external magnetic field **H** (*a*) in the plane of the MM-

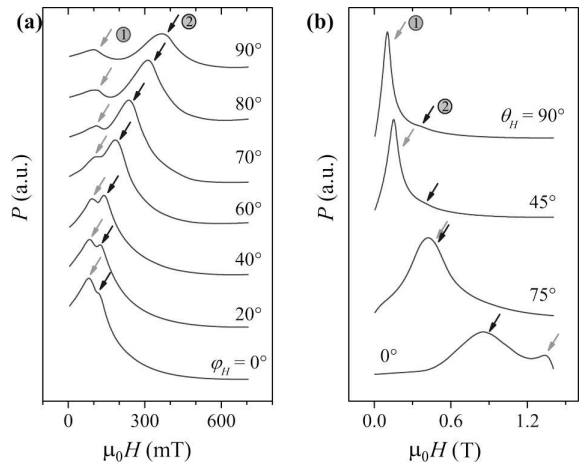

Fig. 2. Angular dependences of the FMR absorption spectra obtained, when the external magnetic field **H** is oriented in the plane of the MM-11N ribbon (*a*) and in the plane including the normal **n** to the ribbon surface (*b*) (see Fig. 1)

11N ribbon (panel *a*) and in the plane of the normal **n** to the ribbon surface (panel *b*) are shown (see Fig. 1).

The angular dependences of the FMR spectra measured in the MM-11N ribbon plane (Fig. 2, *a*) demonstrate two distinct lines of resonance absorption. Those lines evidently correspond to two types of coexisting ferromagnetic regions with different magnetic properties: the amorphous (FM1) and nanocrystalline (FM2) ones. The different characters of the angular dependences for two resonance lines testify that those two regions have absolutely different magnetic anisotropies. The resonance field of line *1* is practically independent of the magnetic field orientation, which evidences that region *1* is magnetically isotropic. At the same time, the angle dependence of the resonance field of line *2* exhibits the pronounced 180° symmetry, which testifies to the uniaxial magnetic anisotropy in region *2*, with the easy anisotropy anisotropy axis coinciding with the direction of an electric current applied at the annealing (ribbon axis). Thus, resonance line *2* corresponds to those FM regions in the nanocrystalline phase (FM2), for which the magnetic anisotropy was expected. On the other hand, line *1* corresponds to magnetically isotropic amorphous regions (FM1).

The FMR spectra registered in the "perpendicular" configuration (Fig. 2, *b*) also reveal two resonance lines, whose positions vary depending on the orientation of the field **H**. The observed angular dependences are a result of the sample shape anisotropy, because the MM-11N samples were cut out from a ribbon. The spectrum marked as $\theta_{\rm H} = 90°$ in Fig. 2, *b* corresponds to the spectrum marked as $\varphi_{\rm H} = 90°$ in Fig. 2, *a*, which allows an unambiguous correspondence to be established between the resonance lines measured in two configurations. A detailed analysis of the line shift in the spectra corresponding to the "perpendicular" configuration revealed the position exchange between lines *1* and *2*, when line *2* is observed at lower fields than line *1* at the angle $\theta_{\rm H} = 0°$. Since the resonance field is proportional to the sample magnetization [see expressions (1)], this behavior proves that regions *2* have a lower effective magnetization than regions *1*.

The different relative intensities of resonance lines, which were revealed for two measurement configurations, should be associated with different values of the absorption coefficient in two FM regions of the MM-11N sample, which depends on the orientation of the magnetic component of the microwave field with respect to the ribbon plane: either perpendicular (Fig. 2, *a*) or parallel (Fig. 2, *b*) to the ribbon plane. Therefore, the intensities of resonance lines cannot be used to evaluate the volume fractions of the corresponding regions. At the same time, X-ray structural data [18] demonstrate that the nanocrystalline phase, which corresponds to resonance line *2*, comprises about 75 vol%.

Figure 3 exhibits the angular dependences of the FM resonance fields for the two detected resonance lines *1* and *2* registered in two measurement configurations. The dependences were calculated using the numerical description of experimental spectra with the help of the Lorentzian function. The obtained angular dependences of the resonance fields were characterized in the framework of the Smit–Beljers FMR formalism (2). The calculated angular

Magnetic parameters of the FM1 and FM2 regions in a ribbon of MM-11N alloy

Parameter	Region FM1	Region FM2
$M_{\rm eff}$, kA/m	1300	810
$B_{\rm eff}$, T	1.63	1.02
$K_{\rm u}$, kJ/m^3	–	21
$K_{\rm u}^*$, kJ/m^3	1.8	1.8
$g_{\rm eff}$	2.13	1.91

* This value was obtained from the magnetic reversal loop measurements.

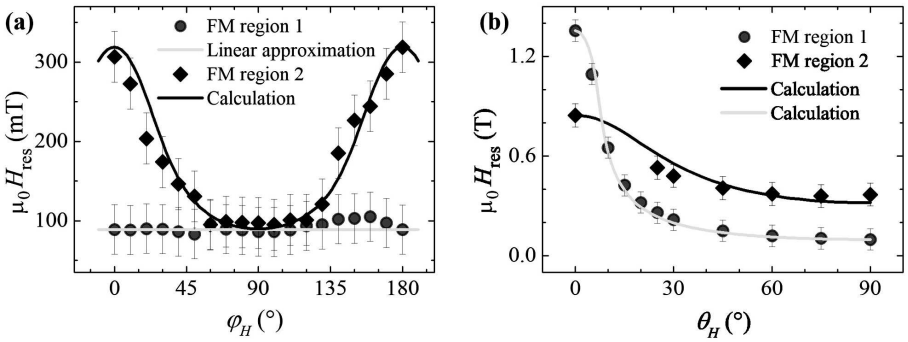

Fig. 3. Angular dependences of the FM resonance fields for two detected resonance lines 1 and 2, when the external magnetic field **H** is applied in the plane of the MM-11N ribbon (*a*) and in the plane including the normal **n** to the ribbon surface (*b*) (see Fig. 1)

dependences of resonance fields are shown in Fig. 3 by solid curves. The calculated dependences describe the experimental results rather well.

The calculations showed that the angular dependences of the resonance field for line *2* in the ribbon plane are governed by the magnetic anisotropy of the "easy axis" type (for comparison, line *1* does not reveal any distinct anisotropy). At the same time, the angular dependences in the "perpendicular" configuration are governed by the sample shape anisotropy for both lines. By fitting the experimental data, the values of the effective magnetization M_{eff} and the effective field of uniaxial anisotropy H_{ua} were calculated for each of the two regions. It should be noted that the results exhibited in Figs. 3, *a* and *b* were calculated together and are characterized by the same parameter values for two measurement configurations.

In Fig. 4, a comparison is made for the values of the demagnetization field (magnetic induction), $4\pi M_{\text{eff}}$, obtained for two FM regions and the uniaxial anisotropy field H_{ua} obtained for the FM2 region. The significantly larger value for the demagnetization field in the FM1 region should be associated with its much higher magnetization as compared with that in region FM2. In turn, the anisotropy field H_{ua} obtained for the FM2 region can be recalculated into the uniaxial anisotropy constant as follows: $K_{\text{u}} = 1/2\mu_0 M_{\text{eff}} H_{\text{ua}}$.

In Table, the values of the effective magnetization $4\pi M_{\text{eff}}$ and the magnetic induction B_{eff} obtained for the FM1 and FM2 regions are compared, as well as the values of the anisotropy constant K_{u} obtained on the basis of the FMR measurements and the measurements of the dynamic hysteresis loop. The

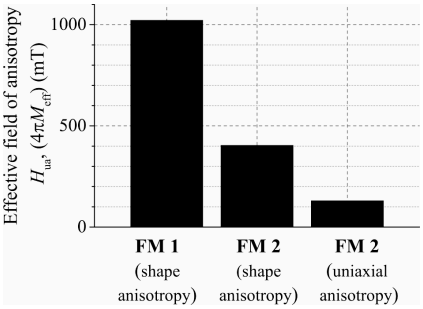

Fig. 4. Effective anisotropy fields of the ferromagnetic FM1 and FM2 phases in the ribbon of MM-11N alloy

value $K_{\text{u}} = 21$ kJ/m^3 obtained from the FMR data for the FM2 regions does not agree with the value $K_{\text{u}} = 1.8$ kJ/m^3 obtained from the dynamic hysteresis loop taking place at the magnetic reversal of the core wound from the examined ribbon. In the latter case, the value of K_{u} was calculated from the area above the reverse magnetization loop (measured at a frequency of 1 kHz) by numerically integrating the quantity $H\Delta B$. The discrepancy between the quantitative estimates obtained from the resonance and magnetometric measurements testifies to a complicated magnetic state of the alloy, which is a subject of further researches.

4. Conclusions

Using the ferromagnetic resonance method, the resonance properties of nanocrystalline ribbons fabricated from $Fe_{73}Cu_1Nb_3Si_{16}B_7$ alloy and annealed with the help of an electric current under a tensile stress of 180 MPa have been studied. The angular dependences of the corresponding FMR spectra re-

vealed two angles of a resonance absorption, which correspond to ferromagnetic regions of two types with different anisotropic behaviors. The ferromagnetic regions of the first type are weakly anisotropic, whereas the regions of the second type are characterized by a pronounced uniaxial magnetic anisotropy. On the basis of the FMR formalism, the magnetic parameters of the ferromagnetic regions are calculated. A conclusion is made that the regions of the first type correspond to the amorphous phase, and the region of the second type to the nanocrystalline one. The both phases coexist in the annealed samples fabricated from the amorphous alloy.

The work was carried out in the framework of the projects Nos. 0119U100469 and 0118U003265 of the National Academy of Sciences of Ukraine, and the project No. 0119U101609 of the Target Preparation Branch of the Taras Shevchenko National University of Kyiv at the National Academy of Sciences of Ukraine.

1. Y. Yoshizawa, S. Oguma, K. Yamauchi. New Fe-based soft magnetic alloys composed of ultrafine grain structure. *J. Appl. Phys.* **64**, 6044 (1988).
2. K. Hono, K. Hiraga, Q. Wang, A. Inoue, T. Sakurai. The microstructure evolution of a $Fe_{73.5}Si_{13.5}B_9Nb_3Cu_1$ nanocrystalline soft magnetic material. *Acta Metall. Mater.* **40**, 2137 (1992).
3. V.V. Nemoshkalenko, L.E. Vlasenko, A.V. Romanova, A.P. Brovko, V.V. Maslov, V.K. Nosenko, Y.U. N. Petrov. Nanocrystal structure at the stage prior to crystallization of amorphous $Fe_{73.5}Si_{13.5}B_9Cu_1Nb_3$. *Metallofiz. Noveish. Tekhn.* **20**, 22 (1998).
4. V.V. Maslov, V.K. Nosenko, L.E. Tapanenko, A.P. Brovko. Nanocrystallization in FINEMETs. *Phys. Met. Metallogr.* **91**, 474 (2001).
5. R. Hono. Nanoscale microstructural analysis of metallic materials by atom probe field ion microscopy. *Mater. Sci.* **47**, 621 (2002).
6. G. Herzer. Anisotropies in soft magnetic nanocrystalline alloys. *J. Magn. Magn. Mater.* **294**, 99 (2005).
7. D. Azuma, R. Hasegawa, S. Saito, M. Takahashi. Effect of residual strain in Fe-based amorphous alloys on field induced magnetic anisotropy and domain structure. *J. Appl. Phys.* **113**, 17A339 (2013).
8. S. Flohrer, R. Schäfer, J. McCord, S. Roth, L. Schultz, F. Fiorillo *et al.* Dynamic magnetization process of nanocrystalline type wound cores with transverse field-induced anisotropy. *Acta Materialia.* **54**, 4693 (2006).
9. L. Kraus, K. Závěta, O. Heczko, P. Duhaj, G. Vlasák, J. Schneider. Magnetic anisotropy in as-quenched and stress-annealed amorphous and nanocrystalline $Fe_{73.5}Cu_1Nb_3Si_{13.5}B_9$ alloys. *J. Magn. Magn. Mater.* **112**, 275 (1992).
10. G. Herzer. Creep induced magnetic anisotropy in nanocrystalline Fe–Cu–Nb–Si–B alloys. *IEEE Trans. Magn.* **30**, 4800 (1994).
11. B. Hofmann, H. Kronmüller. Creep induced magnetic anisotropy in nanocrystalline $Fe_{73.5}Cu_1Nb_3Si_{13.5}B_9$. *Nanostruct. Mater.* **6**, 961 (1995).
12. G. Herzer, V. Budinsky, C. Polak. Magnetic properties of nanocrystalline FeCuNbSiB with huge creep induced anisotropy. *J. Phys.: Conf. Ser.* **266**, 012010 (2011).
13. T. Yanai, K. Takagi, K. Takahashi, M. Nakano, Y. Yoshizawa, H. Fukunaga. Fabrication of Fe-based ribbon with controlled permeability by Joule heating under tensile stress. *J. Magn. Magn. Mater.* **320**, e833 (2008).
14. T. Yanai, T. Ohya, K. Takahashi, M. Nakano, Y. Yoshizawa, H. Fukunaga. A new fabrication process of Fe-based ribbon with creep-induced anisotropy. *J. Magn. Magn. Mater.* **290–291**, 1502 (2005).
15. E. Csizmadia, L. K. Varga, Z. Palánki, F. Zámborszky. Creep or tensile stress induced anisotropy in FINEMET-type ribbons? *J. Magn. Magn. Mater.* **374**, 587 (2015).
16. F. Alves. Flash stress annealings in nanocrystalline alloys for new inductive components. *J. Magn. Magn. Mater.* **226–230**, 1490 (2001).
17. H. Fukunaga, H. Tanaka, T. Yanai, M. Nakano, K. Takahashi, Y. Yoshizawa. High performance nanostructured cores for chock coils prepared by using creep-induced anisotropy. *J. Magn. Magn. Mater.* **242–245**, 279 (2002).
18. A. Nosenko, T. Mika, O. Rudenko, Y. Yarmoshchuk, V. Nosenko. Soft magnetic properties of nanocrystalline $Fe_{73}B_7Si_{16}Nb_3Cu_1$ alloy after rapid heating under tensile stress. *Nanoscale Res. Lett.* **10**, 136 (2015).
19. C. Kittel. On the theory of ferromagnetic resonance absorption. *Phys. Rev.* **73**, 155 (1948).
20. A.Ya. Blank, M.I. Kaganov. Ferromagnetic resonance and plasma effects in metals. *Sov. Phys. Uspekhi.* **10**, 536 (1968).
21. J. Smit, H.G. Beljers. Ferromagnetic resonance absorption in $BaFe_{12}O_{19}$, a highly anisotropic crystal. *Phillips Res. Rep.* **10**, 113 (1955).

Received 03.06.19.
Translated from Ukrainian by O.I. Voitenko

А.М. Погорілий, Д.М. Поліщук, О.І. Товстолиткін, А.Ф. Кравець, В.О. Заморський, А.В. Носенко, В.К. Носенко

РЕЗОНАНСНІ ВЛАСТИВОСТІ ТА МАГНІТНА АНІЗОТРОПІЯ НАНОКРИСТАЛІЧНОГО СПЛАВУ $Fe_{73}Cu_1Nb_3Si_{16}B_7$

Р е з ю м е

Методом феромагнітного резонансу досліджено резонансні властивості нанокристалічних стрічок сплаву $Fe_{73}Cu_1Nb_3Si_{16}B_7$, відпалених електричним струмом під розтягувальним напруженням 180 МПа. Виявлено, що після відпалу в сплаві співіснують два типи феромагнітних областей з різною анізотропною поведінкою. Перша з них є аморфною і слабко магнітно анізотропна, тоді як друга область характеризується яскраво вираженою одноосною магнітною анізотропією і відповідає нанокристалічній фазі. Зроблено кількісні оцінки магнітних параметрів двох магнітних фаз сплаву.